

Experimental evaluation of the energy responsible for the crack advancing

Daniel Vavřík^{1,2a}, Ivan Jandejsek^{1b}

¹ Institute of Theoretical and Applied Mechanics AS CR, v. v. i., Prosecka 76, Prague 9, Czech Republic

² Czech Technical University in Prague, Institute of Experimental and Applied Physics, Horska 3a/22, Prague 2, Czech Republic

^a vavrik@itam.cas.cz, ^b jandejs@itam.cas.cz

Keywords: Fracture process zone, Digital radiography, Digital Image Correlation.

Abstract. Many high performance ductile structures in civil engineering, automotive, aerospace and electrical industries are manufactured from high ductile thin wall materials. The mechanical behaviour of such materials is different from that of bulk (thick wall) materials. It is well known that measured value of fracture toughness strongly depends on many factors, namely geometry and type of loading. The existence of the plastic region in crack front is generally taken as a reason for dependence of fracture toughness on the body geometry. As appropriate determination of the fracture toughness evaluation of the energy responsible for fracture advancing can be considered. For such evaluation, the knowledge of several physical quantities is necessary: crack shape and processing zone behaviour, strain-stress field and plastic deformation. Combination of several experimental methods - computed tomography, Digital Image Correlation and strain gauge measurements were employed for this purpose.

Introduction

A complex experiment was carried out with 2 mm thick specimen made of aluminum alloy containing stress concentrator in the form of sharp V-Notch (MT configuration). For precise evaluation of the full-field strain distribution the enhanced optical Digital Image Correlation (DIC) method in conjunction with strain gauge measurement was employed. It was proven in the past [1], that crack is tunneling (and slanting) even for such thin material as used in our experiment. Therefore the Fracture Process Zone (FPZ) is not directly visible from the surface and optical observation may underestimate the crack length. In this work, the crack length and FPZ shape was measured using digital transmission radiography from these reasons.

Calculations of the stress, plasticity and elastic/plastic work was done using experimental DIC measurement of the full field strain distribution. These calculations are based on well-known continuous mechanics equations where FPZ area is not taken into account because non-continuous material is inside of this area. It is supposed that energy equal to the difference between external and inner works (plastic, elastic and thermal) corresponds to energy dissipated by the FPZ and crack evolution. Thermal energy dissipation was not taken into account for the energy balance calculation in this paper.

It was observed, that plastic zone and FPZ developed smoothly during loading, thereafter evolution of this region switched into slow evolution of transversal slanting crack after reaching maximal loading force.

Experiments

Tested material and specimens. The high ductile Al-alloy (AlMg5: equivalent to EN10204.H321) was used for preparation of a flat specimen (170x50x2 mm) with central 30 mm long slit ended by sharp V-notches. The modulus of elasticity E and Poisson's ratio ν of the material is 69 GPa and 0.3, respectively. The yield point $R_{p0.2}$ of the material is 215 MPa and its strength is 350 MPa.

Speckle pattern was prepared on the specimen surface for optical measurement of the displacement field using Digital Image Correlation technique. Three strain gauges rosettes were glued on the other side.

Experimental setup. The specimen was loaded in tension using a tabletop loading device [2]. The specimen was loaded in uniaxial tension by grips displacement with velocity $0.44 \mu\text{m}/\text{sec}$ until initial V-notch prolonged to several millimetre long crack. The specimen surface with random speckle pattern was optically observed by a 15 MPixel camera via silicate mirror. Optical data are used for calculation of the stress/strain field using DIC method [3]. The mirror allows keeping the camera outside of the X-ray beam, which was used for radiographic observation of the crack and FPZ evolution. See [4] for more details about X-ray setup. Strain gauges data were used for reference measurement for DIC.

Results

Data acquisition. Optical images in raw format were acquired with frame rate 0.2 f/s. An example of the optical image at the end of experiment is in Fig. 1 left. A detail of the V-notch is in Fig. 1 middle (only one half of the slit was recorded). The crack, visible on the surface (1 mm length), is depicted in Fig. 1 right.

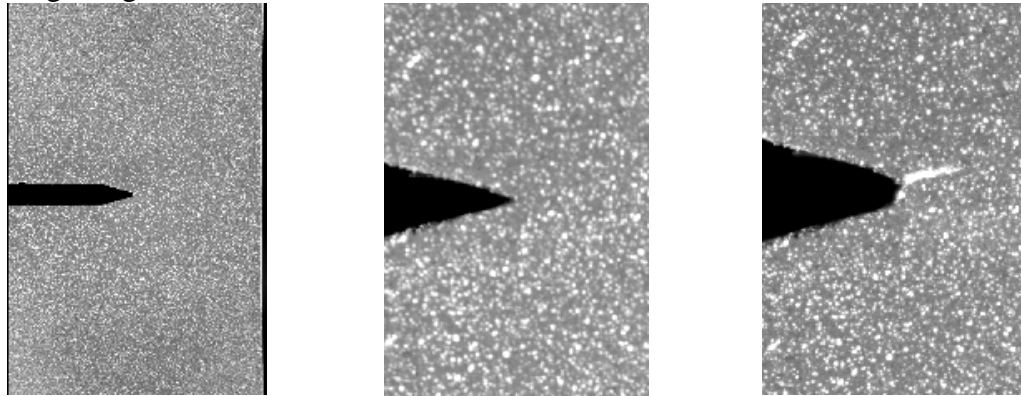


Fig. 1. Optical images of the specimen left. A detail of the sharp V-notch middle (several microns radius). A crack growing from the blunted notch is visible on the specimen surface, right. Both details have the same magnification. Deposited speckle pattern is used for DIC calculations.

Since relatively small movement of the specimen in the loading device during loading is influencing precision of the DIC calculation, strain gauges were employed for the correction of this movement. Three strain gauges rosettes are sufficient for this task.

Radiograms were recorded with frame rate 0.5 f/s. The radiogram from the end of the experiment is shown in Fig. 1 left. It is easy to recognize strain gauges in left side of this image. The detail of 2.4 mm long crack is visible in Fig. 1 right (coordinates $[0,0]$ correspond to the initial crack tip position). This crack is not imaged as straight because it was slanting from the slit direction. Approximately one millimeter long FPZ is also visible in this image. Note that boundary between FPZ and original material is not sharp as can be expected. The crack is actually longer than it looks from the optical image of the surface due to its tunneling.

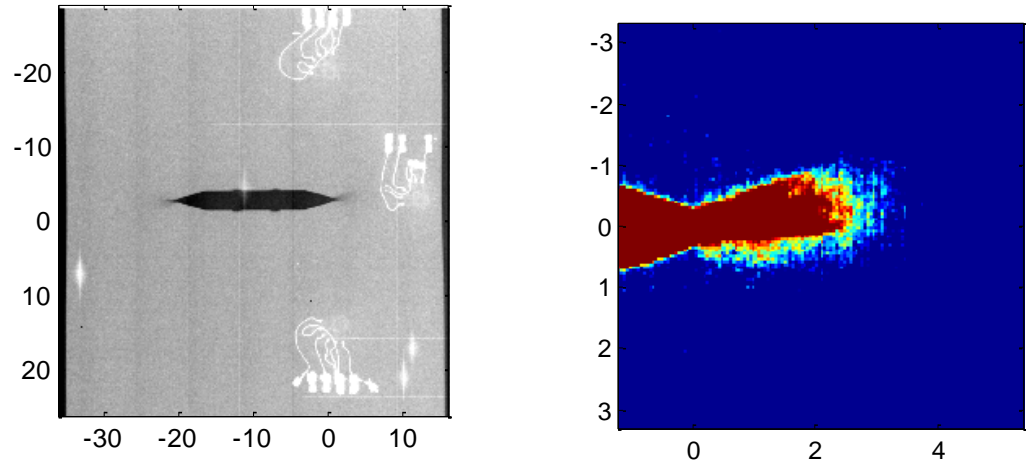


Fig. 2. Radiogram of the specimen at the end of experiment left. Strain gauges are well visible. Detail of the crack (red color) and related FPZ right (from red to light blue).

Data from loading device dynamometer were acquired with frequency 2Hz. Displacements of the grips were counted by the loading device thanks to known transmission ratio of its mechanism. Related force vs displacement graph is plotted in Fig. 3.

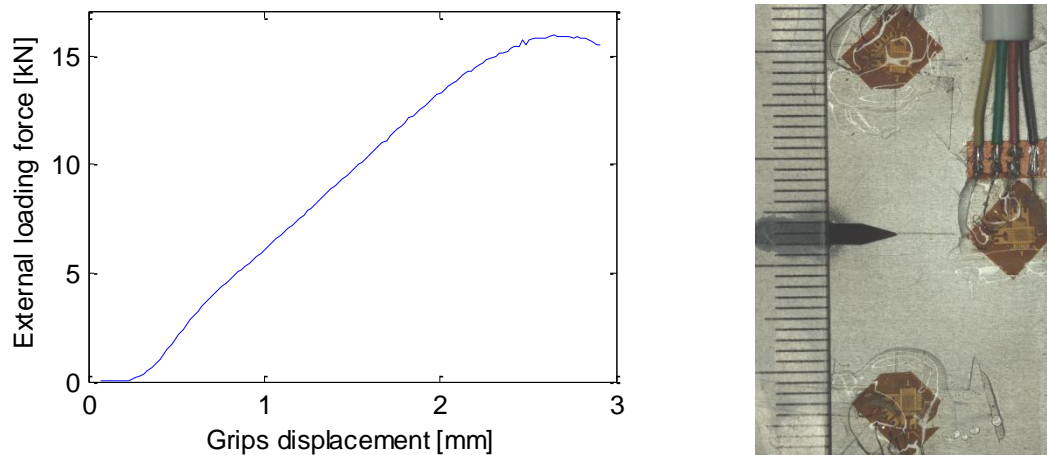


Fig. 3. Loading record left. Photography of the specimen back side right. Strain gauges rosettes are imaged as well as millimetre scale measuring rule.

Data processing. Optical data acquired during whole loading experiment were used for calculation of the full displacement/strain fields employing DIC tools. An adaptive meshing was utilized for definition of DIC subset initial positions to describe high strain gradient in the vicinity of the stress concentrator while strains are calculated with high precision also in places with low gradients (prevalently elastic deformation). This mesh is plotted in Fig. 4 left. The strain fields ε_1 , ε_2 measured by DIC method were corrected using data from strain gauges rosettes (see Fig. 3 right for their positions), where influence of rigid body motion on DIC strain fields measurement was suppressed (specimen movement during loading may change focal plane of the optical system). Corrected strain fields were consequently mapped onto fine and regular orthogonal grid. Such strain field ε_1 at the end of the loading is depicted in Fig. 4 middle as example; note that V-notch area is not eliminated, consequently virtual strains are inside of this area (contrary V-notch is masked for energy calculations). Original notch tip has coordinates [0,0].

Assuming plane stress, incremental Prager–Ziegler plasticity theory and isotropic hardening rule, stress and plastic strain fields were calculated from the measured strains. Plastic and elastic internal works were calculated as well [5]. Integral external work for all loading levels was obtained using DIC displacement data and computed stress fields. External works fractions were numerically integrated on the path depicted by blue color in Fig. 4 left.

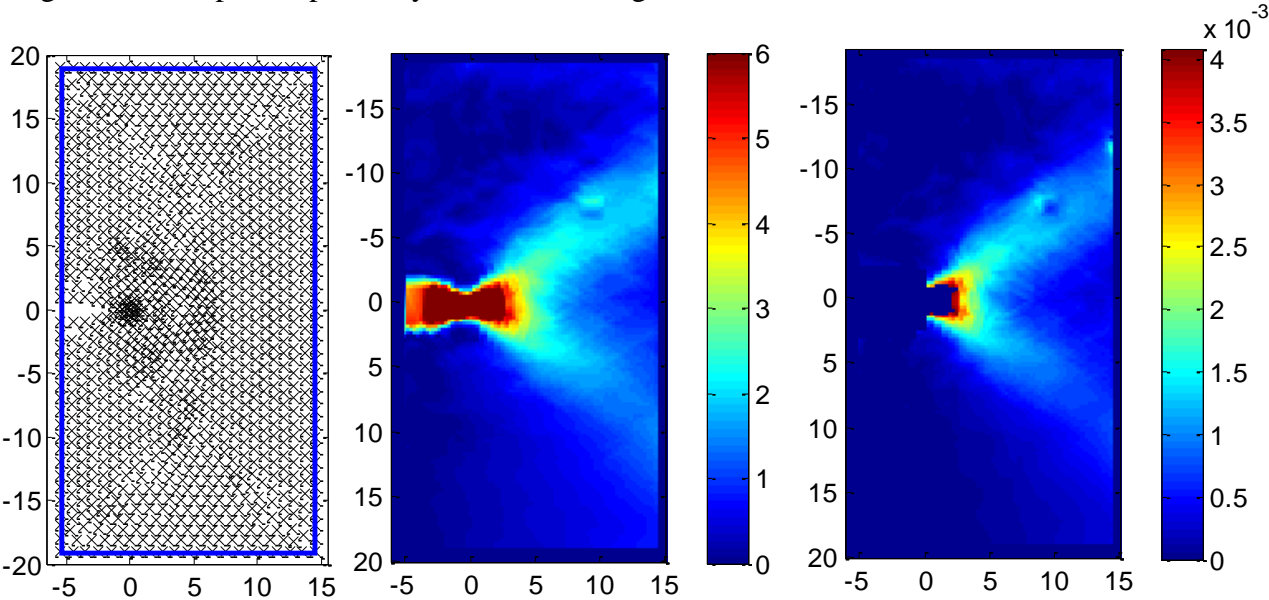


Fig. 4. Adaptive mesh defining DIC subset positions left. Strain field ϵ_1 middle (% scale). Plastic work distribution right (in Joule scale).

Comparing radiographic data and plastic strain intensity it was found that some critical value of the plastic strain intensity exists, which can be taken as crack/FPZ indicator. Note, if crack or FPZ is presented inside of the specimen, significantly higher strains are measured on the specimen surface. The critical value of the plastic strain was used for definition of a mask covering FPZ/crack area. As example, plastic work distribution at the end of loading is imaged in Fig. 4 right, where FPZ/crack area is masked (crack/FPZ length is equal to the value obtained from radiographic measurement).

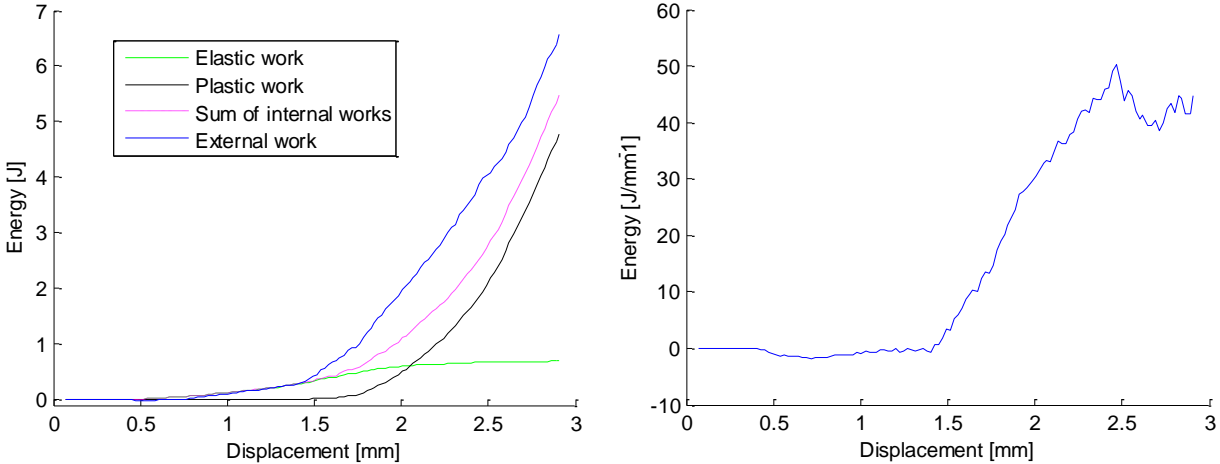


Fig. 5. Evolution of external and internal works during loading is plotted left. Difference between external and internal works right.

Plot of total internal and external works without the masked area is in Fig. 5 left. It is assumed that the difference between such masked internal and external works corresponds to energy dissipated by FPZ and consequent crack evolution. Consequently the difference between total internal and external work evolution was computed, see Fig. 5 right. Values were normalized by the distance between crack tip and external work integration path.

Significant extreme in this difference plot corresponds to the moment, when short (40 μm) main crack developed in the optical data. Subsequent local minimum occurred at the moment, when this short crack blunted. Nevertheless it was followed by slow growing of the main crack.

Conclusions

It was proven that experimentally calculated balance between total external and internal works can identify moment of the crack initiation and growing. This crack growing precedes dissipation energy in the fracture process zone.

Employing of the X-ray radiographic methods is advantageous for identification of the crack and fracture process zone evolution.

Testing of specimens with different constrain factor will be done in next work as well as numerical simulation correlated with experimental results.

Acknowledgement. Financial support from the Czech Science Foundation, project No. 103/09/2101, and RVO 68378297 is gratefully acknowledged.

References

- [1] D. Vavřík, P. Soukup, "Metal Grain Structure Resolved with Table-top micro-Tomographic System", JINST_007P_1011, doi: 10.1088/1748-0221/6/11/C11034 (2011)
- [2] I. Jandajsek, F. Nachtrab, N. Uhlmann, D. Vavřík, "X-ray dynamic defectoscopy utilizing digital image correlation", NIM A, Volume 633, Supplement 1, May 2011, Pages S185-S188, doi: 10.1016/j.nima.2010.06.162 (2011)
- [4] I. Jandajsek, D. Vavřík, Experimental measurement of the J-integral using digital image correlation method, in the proceedings of the European Conference on Fracture 18.. Berlin : Deutscher Verband fur Materialforschung und prufung e.V, Pages. S189-194. ISBN 978-3-00-031802-3. (2010)
- [4] D. Vavřík, J. Dammer, J. Jakůbek, I. Jeon, O. Jiroušek, M. Kroupa, P. Zlámal, "Radiography in Engineering Practice", Nucl. Instr. Methods A, Vol. 633, Suppl. 1, Pages S152-S155, doi:10.1016/j.nima.2010.06.152 (2011)
- [5] D. Vavřík, J. Zemankova, "Crack Instability in Ductile Materials Analyzed by the Method of Interpolated Ellipses", Experimental Mechanics, Vol. 44, Pages. 327-335. ISSN 0014-4851. (2004), DOI: 10.1007/BF02428086